Proceedings of the 2005 IEEE
Engineering in Medicine and Biology 27th Annual Conference
Shanghai, China, September 1-4, 2005

Implementation of High-Temperature Superconducting tapes RF coils for 3T MRI system

In-Tsang Lin [1], Chang-Wei Hsieh [1], Li-Wei Kuo [1], Hong-Chang Yang [2], Ching Yao [3], Wei-Hao Chang [1], Jyh-Horng Chen [1]

[1]Interdisciplinary MRI/MRS Lab, Department of Electrical Engineering, National Taiwan University, Taipei, Taiwan
[2]Department of Physics, National Taiwan University, Taipei, Taiwan.
[3] Division of Medical Engineering Research, National Health Research Institutes, Taipei, Taiwan.

Abstract—**One way to reduce receiving coil noise in MRI scans is using non-resistive high-temperature superconducting (HTS) coils [1]. They show advantages of much lower cost and easier fabrication over HTS thin film coils. In this work, we built a 200mm in diameter $Bi_2Sr_2Ca_2Cu_3O_x$ (Bi-2223) tape HTS RF coil and demonstrated that the SNR of using the HTS tape coil was 2.22 folds higher than that of the traditional copper coil for a phantom MR study. Test results were in agreement with predictions, and the error of predicted SNR gains and measured SNR gains is about 0.9%. The HTS coil can be expected to generate higher SNR gain after optimization. In the future, *in-vivo* experiments will be conducted to farther test the capability of the HTS tape coil. Further applications functional MRI is under investigation to test the power of this HTSC system in our 3T system.**

Keywords—**MRI, Bi-2223, HTS**

I. Introduction

Using superconducting coil in MRI scan can minimize signal loss caused by receiving coil resistance, and significantly raise image SNR. Most HTS RF coils developed so far are film coils [2]. However in the past few years, Bi-based HTS tapes focused on ac power transportation applications have been increasingly developed. When we are interested in larger scale images Bi-based tape coil can be a good alternative of film coils for their easier fabrication, frequency adjustment, flexibility in coil configuration, and much lower cost [3]. In this study, we implemented tape HTS coils and conventional copper coils on Bruker Biospec 3T system and compared the SNR advantage with predictions.

II. Materials and Methods

A. Materials

The $Bi_2Sr_2Ca_2Cu_3O_x$ (Bi-2223) tape coil used for the experiments, provided by Innova Superconductor Technology Co., Ltd. (Beijing, P.R.China)., using the powder-in-tube process, which is embedded in a pure Tin or alloy Tin matrix. The specifications are listed in Table I.

The thickness and width of the raw HTS tape is about 0.23 mm and 4.1 mm respectively, with a tin alloy sheath of thickness about 10 μm to provide mechanical support for the HTS composition [4].

TABLE I
General specification of Bi(2223) tapes.

Critical Temperature	110K
Critical Current (*Ic*)	$\geq$ 85A (77K, self-field)
Engineering Critical Current Density (*Je*)	$\geq 9000\ A/cm^2$
Critical Magnetic Field	~210T
Width	4.10mm $\pm$ 0.10mm
Thickness	0.230mm $\pm$ 0.10mm
Structure	Multi-filamentary
Max. Tensile Stress	100 MPa (5% *Ic* Degradation)
Min. Bending Radius	30 mm (5% *Ic* Degradation)

Normally, an HTS tape has a tin sheath (Sn or Sn alloy) of thickness to increase its flexibility and strength for ac power applications. According to the formulation of the skin depth:

$$\delta = \sqrt{\frac{2\rho}{2\pi f \mu_R \mu_0}} \quad (1)$$

where ρ is the resistivity of the material, f is the frequency of the operating frequency, μ_R is the relative permeability, and μ_0 is the permeability of the free space. The skin depth of Sn at the RF region varies from about 15 μm at 125 MHz to about 150 μm at 1.25 MHz, which is bigger than the sheath thickness of the tape. So that it won't completely screen of the superconducting phase from the RF signal, but it is necessary to dissolve the outer Sn or Sn alloy sheath of the tape to generate better performance. The eventual coating including ceramic coating or a varnish coating can be removed carefully to establish electrical contacts. Coating can be removed cautiously by mechanical polishing using e.g. silicon carbide 800 polishing paper or the copper brush. The wire must be on a flat support during polishing in order to avoid straining. When soldering the HTS wires, it is commonly believed that longer splice will result in a smaller electrical resistance. Additionally, the solder temperature must be kept below $300\ ^0C$.

To build the RF surface coil, the tape has to be bent into a simple circle loop with a diameter larger than the critical diameter of the tape, as shown in Table I, otherwise its critical current will decrease. A non-magnetic capacitor (American Technical Ceramics, US) with high Q (>1000) is soldered directly at both ends of the tape to form an LC resonant loop. The resonant frequency of the surface coil can be determined by

$$f_0 = \frac{1}{2\pi\sqrt{LC}} \quad (2)$$

where f_0 is the resonant frequency of the surface coil, L is the inductance of the loop, and C is the capacitance of the capacitor, which can be chosen to obtain the specific resonant frequency required. In order to test the capability of the HTS RF tape coils, both copper and Bi-2223 were used to be the surface coil with the same size. Differ from the capacitor tuning and matching circuit used in the copper surface coil, mutually inductive coupling between the HTS receiver and the pick-up coil was used [5]-[6]. In Fig. 1, L_1 is the matching coil inductance and L_2 is the surface coil inductance, the input impedance

$$Z_{in} \cong j\omega L_1 + (\omega k L_1 Q / (1 + 2\, jQ\,(\delta\omega / \omega_c))) \quad (3),$$

where $\omega_c = 1/\sqrt{L_2 C_2}$ and k is the coupling constant. In order to create the pure resistive impedance ω_c of 50 ohm at Larmor frequency, the coupling constant k must be set as the appropriate value and has to be offset from the Larmor frequency to compensate the reactance created by the inductive loop. A trimmer capacitor was used in the signal pick-up loop and tuned to the value $C_1 = 1/\omega_0^2 L_1$, so that the imaginary part in Z_{in} from (3) was cancelled out of the resonant frequency. Thus pure resistive impedance $Z_{in} \equiv Qk^2\omega_0 L_1$ could be generated at the coil resonance. We use the above method to design our experiment setup (Fig. 2).

B. *Quality factor*

Quality factor is also a very important parameter to estimate the resistive loss of the RF coil and other losses. It is defined as the resonant frequency times the stored field energy divided by the power loss per circle of RF, as shown in (4) [7]

$$Q = \omega \frac{average\ \ stored\ \ energy}{energy\ \ loss\ \ per\ \ cycle}\bigg|_{\omega=\omega_0} \quad (4)$$

For an LC resonant loop (surface coil), its Q is often given by

$$Q_0 = Q_c = \frac{f_0}{\Delta f} = \frac{\omega_0}{\Delta\omega} = 2\pi f_0 \frac{L}{R} = \omega_0 \frac{L}{R} = \frac{1}{2\pi f_0 RC} \quad (5)$$

where f_0 and ω_0 are resonant frequency and resonant angular frequency of the loop, respectively, Δf or Δω are the bandwidth of the resonant frequency at -3dB, L is the inductance of the loop, C is the capacitance, and R is the total resistance given by the sum of the resistance of the coil itself and the equivalent resistance caused by the loaded sample. Tuning, matching and signal pick-up were done by adjusting relative positions of signal pick-up coil and tune a variable trimmer capacitor to cancel out the imaginary part in Zin. Before imaging the coils were tuned to the resonant frequency of 125.3 MHz and matched to the standard preamplifier of 50 Ω. Coils' frequency responses and Q-values were measured with a Hewlett Packard-8751A Network Analyzer using the S_{11} mode. The S_{11} response is basically the ratio of the reflected power to the total transmitted power by the Network Analyzer via the signal pick-up coil [8]. The Q value was then given by the ratio of the resonance frequency divided by the -3dB frequency bandwidth [8].

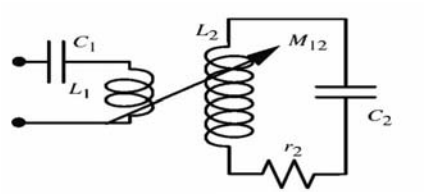

Fig. 1 Matching & signal pick-up coil with variable tuning trimmer capacitor C_1. Adjusting the capacitor C_1, so that the imaginary part in Z_{in} as cancelled out of the resonant frequency.

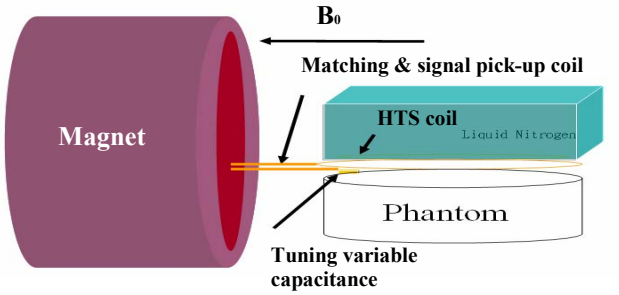

Fig. 2 The system setup of the phantom experiment at 3T, where the matching & signal pick-up coil with a tuning variable capacitance was put in the middle of the HTS tape coil and the phantom.

C. *SNR of a MRI System*

The SNR as detected by the RF coil can be written as [9]

$$SNR = \frac{\xi}{\sigma} = \omega \frac{M_0 V_s}{\sqrt{4k_B \delta f}} \frac{B_1 \cos\omega_0 t}{\sqrt{R_c T_c + R_s T_s}} \quad (6)$$

Where R_c and R_s are the resistance of coil and sample, and T_s are the temperature of coil and sample, ω is the resonant frequency, B_0 is the static magnetic field, B_1 is the induction coefficient that represents the magnetic field produced by the coil per supplied unit current. M is the magnetization, V_s is the voxel volume, δf is the system bandwidth, k is the

Boltzman's constant. From (6) we can find the relation between SNR and coil/sample resistance is

$$SNR \propto \frac{B_1}{\sqrt{R_c T_c + R_s T_s}} \tag{7}$$

From the above relation we can calculate the SNR gain that can be achieved by employing HTS coils as [9]

$$SNR^{gain} = \frac{SNR^{sup\ ercon}}{SNR^{copper}} = \sqrt{\frac{R_c^{copper} T_c^{copper} + R_s T_s}{R_c^{sup\ ercon} T_c^{sup\ ercon} + R_s T_s}}$$

$$= \sqrt{\frac{\alpha R_c^{copper} + R_s}{\alpha R_c^{sup\ ercon} + R_s}} \tag{8}$$

where $\alpha = T_c / T_s \sim 0.263$ and are the resistance of copper and superconducting coils, Rs is the resistance of the imaging sample. From the relation [10]

$$Q_{unloaded} = Q_{loaded}(1+\kappa) \tag{9}$$

we can find that

$$\kappa = \frac{Q_{unloaded}}{Q_{loaded}} - 1 = \frac{R_c + R_s}{R_c} - 1 = \frac{R_s}{R_c} \tag{10}$$

Then we have $R_s = \kappa^{copper} R_c^{copper} = \kappa^{sup ercon} R_c^{sup ercon}$, and SNR^{gain} in (8) becomes

$$SNR^{gain} = \sqrt{\frac{\alpha R_c^{copper} + \kappa^{copper} R_c^{copper}}{\alpha R_c^{sup\ ercon} + \kappa^{sup\ ercon} R_c^{sup\ ercon}}}$$

$$= \sqrt{\frac{(\alpha + \kappa^{copper}) R_c^{copper}}{(\alpha + \kappa^{sup\ ercon}) R_c^{sup\ ercon}}}$$

$$= \sqrt{\frac{(\alpha + \kappa^{copper}) \kappa^{sup\ ercon}}{(\alpha + \kappa^{sup\ ercon}) \kappa^{copper}}} \tag{11}$$

So we can calculate the estimated SNR gain of the HTS coil from the Q-values we measured.

III. RESULTS

A 5-in. Bi-2223 tape RF receiving coil for 0.21T low field MRI has been demonstrated and a 3-fold SNR improvement has been obtained over the room temperature copper coil by Cheng et al. [11]. However, SNR improvement with HTS tape coils applied to high field may have more significance because high field MRI has become the mainstream. A 50mm diameter Bi-2223 tape RF receiving coil for 1.5T MRI has been demonstrated and a 1.36-fold SNR improvement has been obtained over the room temperature copper coil by Yuan et al. [12]. Now our main magnetic field is 3T instead of 1.5T. A 200mm diameter HTS tape surface coil was demonstrated for the first time for phantom imaging at 3T. Accounting for the safety issue, phantom imaging was carried out instead of ***in vivo*** imaging. The sample is a 10cm diameter spherical phantom filled with 10mM $CuSo_4$ solution.

Before the imaging experiment, *Q*s of the coils were measured by mutual coupling method with an HP 8751A network analyzer [13]. Note that *Q*s of the coils had to be measured out of the magnet because any electric devices were not allowed to operate in the scanner room. The predicted SNR gains was estimated by inserting the κ values into (11). The results of the measurements were listed in Table II.

MR experiments were performed on the Bruker Biospec 3T system (Bruker, Germany). The HTS tape coil and copper surface coil were made in 200mm diameter and placed at the same position inside the cryostat. Different power settings were determined for coils by stepping through a range of transmit attenuation values in the prescans. The optimum transmitted power was set with both HTS coil and copper coils in order to maximize the signal amplitude. All images were acquired by using the fast spin echo sequence with TR/TE = 4000/70ms and NEX=1. The FOV, the slice thickness and acquisition matrix size were 25cm · 25cm, 4mm and 256 · 256 respectively. The in-plane resolution was 976 um and the slice thickness was 4 mm. The coronal phantom images obtained with these coils were taken from the plane about 3.2cm depth away from the coils and were shown in Fig. 3. SNR between the cortical regions and the background noise of both images were calculated to compare the performance of HTS and copper coil. The SNR of using the HTS tape coil was 256, 2.22 folds higher than that of using the copper coil, which is 115.

TABLE II
Quality factors for HTS at 77K and copper coil at room temperature (Cu), ul:unloaded, l:loaded (outside magnet)

	Q_{ul}	Q_l	κ	SNR Gain (predicted)
HTS	3227	2521	0.28	224.4%
Cu	1000	970	0.03	

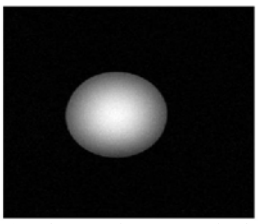

(a) Phantom image acquired from copper coil

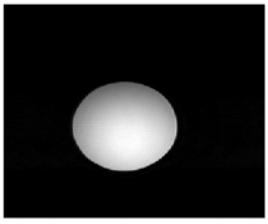

(b) Phantom image acquired from HTS coil

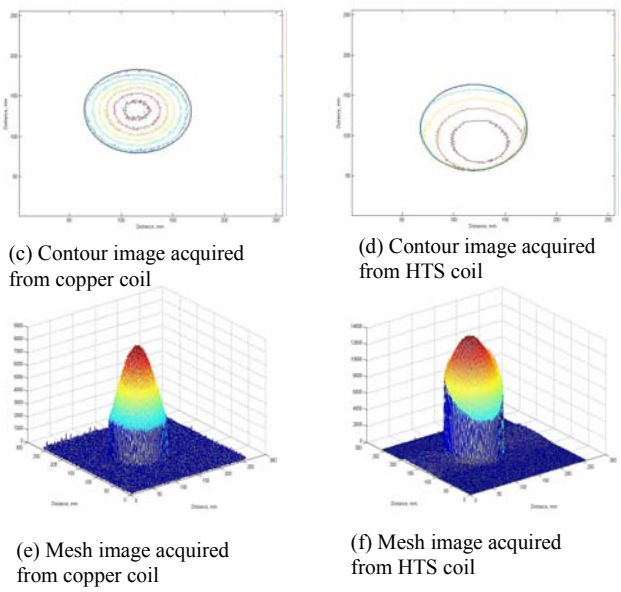

(c) Contour image acquired from copper coil

(d) Contour image acquired from HTS coil

(e) Mesh image acquired from copper coil

(f) Mesh image acquired from HTS coil

Fig. 3. Coronal phantom images, contour images comparison, and mesh images comparison by Bruker fast spin-echo sequence. The background noise of mesh image acquired from HTS coil is lower than copper coil significantly.

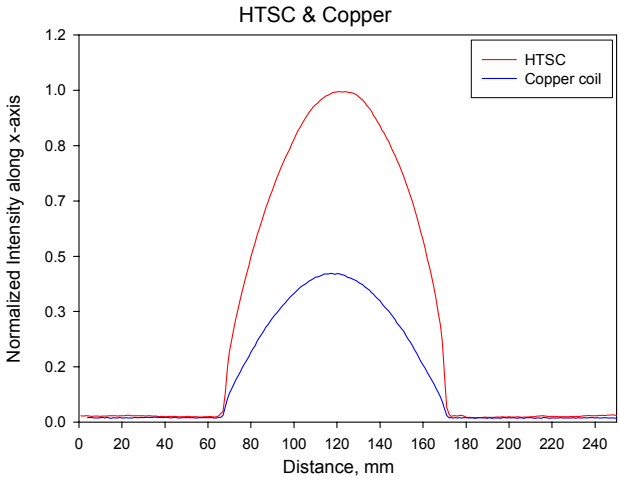

Fig. 4 Plots of intensities along the horizontal axis extracted from phantom images, in which the red, blue curves denote the HTS and copper coil at room temperature, respectively.

Signal intensity along the horizontal axis extracted from images of the phantom with these two coils were plotted and shown in Fig. 4. The results also showed that the image with the HTS tape coil obtained an average SNR improvement of 2.22-fold over the image with the copper coil at room temperature.

V. Conclusion

The advantages of the Bi-2223 tape were easy to fabricate with less cost and relatively easier operation than HTS thin films. A 200mm surface coil for 3T was built and applied to phantom imaging for the first time. Test results were in agreement with theoretical predictions (2.24) and showed a SNR advantage of 2.22 folds over copper coil at room temperature was obtained in the phantom image. The error of predicted SNR gains and measured SNR gains is about 0.9%. The HTS coil can be expected to generate higher SNR gain after optimization. In the future, ***in-vivo*** experiments will be conducted to farther test the capability of the HTS tape coil. Further applications functional MRI is under investigation to test the power of this HTSC system in our 3T system. Many technical issues of HTS tape coils still need to be solved before large-scale applications for routine clinical scans.

References

[1] R. D. Black, T. A. Early, P. B. Roemer, O. M. Mueller, A. Mogro-Campero, L. G. Turner, and G. A. Johnson. "A high-temperature superconducting receiver for nuclear magnetic resonance microscopy". *Science*, 259:793–795, Feb., 1993.

[2] J. R. Miller, S. E. Hurlston, Q. Y. Ma, D. W. Face, D. J. Kountz, J. R. MacFall, L. W. Hedlund, and G. A. Johnson. "Performance of a high-temperature superconducting probe for in vivo microscopy at 2.0 T". *Mag. Reson. Med.*, 41:72–79, 1999.

[3] J. Yuan and G. X. Shen. "Quality factor of bi(2223) high-temperature superconductor tape coils at radio frequency. " *Supercon. Sci. Tech.*, 17:333–336, 2004.

[4] Available: http://www.innost.com

[5] P. L. Kuhns, M. J. Lizak, S. H. Lee, and M. S. Conradi. "Inductive coupling and tuning in nmr probes for in vivo nmr." *J. Magn. Reson*., 78:69–76, 1988.

[6] H-L. Lee, I-T. Lin, L-W. Kuo, H-C. Yang, J-H. Chen "High-Tc Superconducting Receiving Coils for Magnetic Resonance Imaging," *IEEE Trans. Appl. Supercond., 2005*, unpublished.

[7] R. Ludwig, P. Bretchko, RF Circuit Design: Theory and Application, Prentice-Hall, Englewood Cliffs, NJ, 2000, p. 205.

[8] F. E. Terman, "Radio-Engineer's Handbook", Mc-Graw-Hill: New York, (1943)

[9] Jean-Christophe Ginefri et al, "High Temperature Superconducting Surface Coil for In Vivo Microimaging of the Human Skin" *Magn. Res. in Medicine*, **45**, 376-382 (2001)

[10] D. Kajfez and E. J. Hawn. Q-factor measurement with network analyzer. *IEEE Trans. Microwave Theory Tech.*, MTT-32(7):666–670, Jul. 1984.

[11] M.C. Cheng, K.H. Lee, K.C. Chan, K.K. Wong, E.S. Yang, ISMRM (2003) 2359.

[12] J. Yuan, G.X. Shen, Supercond. Physica C 415 (2004) 189–196

[13] J. Yuan, G.X. Shen, Supercond. Sci. Technol. 17 (2004) 333-336.